Aalborg Universitet

Improving Microgrid Frequency Regulation Based on the Virtual Inertia Concept while Considering Communication System Delay

Alizadeh, Gholam Ali; Rahimi, Tohid; Nozadian, Mohsen Hasan Babayi; Sanjeevikumar, P.; Leonowicz, Zbigniew

Improving Microgrid Frequency Regulation Based on the Virtual Inertia Concept while Considering Communication System Delay

Gholam Ali Alizadeh [1], Tohid Rahimi [2],[*] , Mohsen Hasan Babayi Nozadian [2] , Sanjeevikumar Padmanaban [3],[*] and Zbigniew Leonowicz [4]

[1] Department of Electrical and Computer Engineering, Faculty of Ghazi Tabatabai, Urmia Branch, Technical and Vocational University (TUV), Urmia 5716933959, Iran; Alizadeh_88@yahoo.com
[2] Electrical and Computer Engineering Faculty, University of Tabriz, Tabriz 57734, Iran; m.hasanbabayi@tabrizu.ac.ir
[3] Department of Energy Technology, Aalborg University, Esbjerg 6700, DK-9220 Aalborg, Denmark
[4] Faculty of Electrical Engineering, Wroclaw University of Science and Technology, Wyb. Wyspianskiego 27, 50370 Wroclaw, Poland; zbigniew.leonowicz@pwr.edu.pl
[*] Correspondence: rahimitohid@tabrizu.ac.ir (T.R.); san@et.aau.dk (S.P.); Tel.: +98-9361996335 (T.R.)

check for
updates

Abstract: Frequency stability is an important issue for the operation of islanded microgrids. Since the upstream grid does not support the islanded microgrids, the power control and frequency regulation encounter serious problems. By increasing the penetration of the renewable energy sources in microgrids, optimizing the parameters of the load frequency controller plays a great role in frequency stability, which is currently being investigated by researchers. The status of loads and generation sources are received by the control center of a microgrid via a communication system and the control center can regulate the output power of renewable energy sources and/or power storage devices. An inherent delay in the communication system or other parts like sensors sampling rates may lead microgrids to have unstable operation states. Reducing the delay in the communication system, as one of the main delay origins, can play an important role in improving fluctuation mitigation, which on the other hand increases the cost of communication system operation. In addition, application of ultra-capacitor banks, as a virtual inertial tool, can be considered as an effective solution to damp frequency oscillations. However, when the ultra-capacitor size is increased, the virtual inertia also increases, which in turn increases the costs. Therefore, it is essential to use a suitable optimization algorithm to determine the optimum parameters. In this paper, the communication system delay and ultra-capacitor size along with the parameters of the secondary controller are obtained by using a Non-dominated Sorting Genetic Algorithm II (NSGA-II) algorithm as well as by considering the costs. To cover frequency oscillations and the cost of microgrid operation, two fitness functions are defined. The frequency oscillations of the case study are investigated considering the stochastic behavior of the load and the output of the renewable energy sources.

Keywords: frequency stability; load frequency control; communication system delay; virtual inertia

1. Introduction

Microgrids are small power networks that are composed of loads, distributed generations, energy storage resources, telecommunication facilities and other infrastructure [1,2]. These networks are protected from damages resulting from the faults of the upstream network. The stochastic variations of generation units and load profiles [3,4] are common issues in these networks. The availability of different forms of energy storage in microgrids as well as their contribution to electricity markets at

different time periods justify microgrids more economically. These networks are suitable for critical applications such as hospitals and military centers, which require high levels of reliability. Natural disasters and system faults events can rarely affect the performance of these systems [5].

With the increasing penetration of renewable energy technologies in power grids, these grids experience new challenges. In a microgrid, power sources are connected to the network by power electronic converters. These interfaces have very fast transient responses, which reduces the overall inertia of the system. Consequently, low-inertia microgrids are less stable against any electrical disturbances. The imbalance between supply and load leads to frequency fluctuation. This problem, in turn, is aggravated by the presence of renewable energy sources. Renewable energy sources have unpredictable and fluctuating generation modes [6–9]. Fortunately, the energy storage units are capable of functioning as a power source or as load, and therefore can help attenuate the frequency fluctuations by absorbing or supplying power [10–14].

For the stable operation of microgrids, balancing between demand and supply in real time is an essential step, so that the frequency can be constant in its acceptable range. This task can be fulfilled using the load-frequency control mechanism [15]. The microgrid central controller divides the demand power between the power supply sources, thus maintaining the frequency of the system in the acceptable range [16]. Kalantar and Mousavi have studied the dynamical behavior of a hybrid system, which consisted of a wind turbine, microturbine, solar array, and battery according to the genetic algorithm and fuzzy controller [17]. Gao et al. have introduced active topology in its experimental and laboratory sense to control another hybrid system, including a battery and fuel cell [18]. Nayyeri Pour et al. have implemented the PI frequency control method in a local hybrid network composed of photovoltaic, a wind turbine, fuel cell, and super-capacitor. In addition, one PI controller is considered for each source, which determines the reference power of each unit for frequency stabilization by receiving frequency deviation [19]. In reference [20], a fuzzy set and Harmonic Search Algorithm is proposed to adjust the PI controller coefficients in the microgrid in the presence of an electric drive. In reference [21], an optimized fuzzy control system is used to overcome the frequency fluctuations of the microgrid against load and generation uncertainties. One of the modern methods to smooth frequency oscillation and improve the stability of microgrids is virtual synchronous generators [22,23]. In this method, pseudo inertial forces are realized by controlling DGs inverters to emulate the behavior of synchronous generators virtually into microgrids [24]. A Battery/Ultra capacitor hybrid energy storage system is introduced in reference [25] to cover power management and virtual synchronous generator emulation goals. In reference [26], an adaptive control method based on a virtual inertia system with MPC has been presented for frequency oscillation damping by emulating virtual inertia into the microgrid. The virtual inertia control is molded by a first-order transfer function in reference [26]. In reference [27], ultra-capacitor systems are controlled in a way that increases the virtual inertia of the studied microgrid. However, it is important to optimize the ultra-capacitor bank size to avoid extra costs.

On the other hand, with the development of computing and telecommunication systems, communication media are being used to exchange power between the central processing unit and the loads. However, with the increasing penetration of telecommunication networks in the control tasks, the delay between secondary controller and power resources cannot be ignored. Researchers have investigated the stability of the frequency control system in the presence of a time delay in several systems [27–29]. With decreasing communication delay, the cost of the communication infrastructure increases, however the frequency stability remains in a suitable state.

As discussed above, improving the inertia of microgrid and reducing the time delay of the communication system are effective methods to overcome frequency oscillations. However, this approach increases the operation cost of a microgrid. It is essential to select optimum values of time delay and Ultra capacitor size to have acceptable frequency oscillation of a microgrid and operation costs. To sum up, the challenges that discussed in this paper are given as follows:

- To reduce the installation costs, the size of the installed equipment should be minimal, so that the system will not face high costs during its long operation time.

- To enhance the frequency behavior of the microgrid, communicational infrastructure with minimum delays is required to update information quickly.

With considering the challenges that discussed above, this paper aim is determining optimal virtual inertia, comunication delay time and frequency control parameters simultaneously that are not investigated in previous papers. The proposed strategy guarantees frequency stability and decreases the cost of the microgrid's infrastructure. A Minimum ultra-capacitor size and communication delay value are selected in the proposed approach to decrease the cost of the microgrid's infrastructure. Also, the stable and unstable regions for different time delay and virtual inertia values are derived.

Multi-objective optimization methods are used to determine the parameters used in the load-frequency strategies to optimize the several objectives discussed previously [30]. The NSGA-II algorithm is a popular and justified optimizing algorithm [31,32]. Therefore, The NSGA-II algorithm is used in this paper to address the ultra-capacitor size as virtual inertia and the delay of the telecommunications system.

2. Case Study

Here, a microgrid system, which is isolated from the main grid, is considered for this case study. The islanded system consists of power generation, storage units, and telecommunication configurations. Diesel Generator Unit, Fuel Cell Unit, Solar Unit, and Wind Unit are responsible for power generation. The electrolyze unit is also use to absorb extra power. Ultra-capacitors are additionally used to generate and/or absorb power quickly in order to increase the virtual inertia of the network.

The central controller needs frequency information to appropriately order the microgrid power generation and absorption units. As discussed in reference [33], frequency and power information are to be sent or received with a specific time delay by a telecommunications platform, which is very effective for the stability of the microgrid. The communication delay with other delay sources are defined as a measurement delay in reference [34] and applied for primary and secondary controllers. The microgrid mentioned before is shown in Figure 1. Δf is the frequency deviation and input signal of the controller, and the changes in the power generation and storage units as the output of this system. M represents the total inertia of a microgrid. When a difference between the generation and consumption occurs because of the load along with power generation increasing/decreasing, the frequency deviation of the microgrid depends on the inertia value and the load demand. It is assumed that the solar unit has variable and uncontrollable power. The central controller block sets a PI controller output for each power unit. The central controller unit block receives the network frequency information with a delay. The power and frequency information are passed through with a telecommunication system delay. The Diesel Generator Unit, Fuel Cell Unit, and electrolyze unit are equipped with primary and secondary frequency controllers. The Ultra-Capacitor unit participates in primary frequency control using a frequency signal. The parameters of this microgrid and power units are given in Table 1.

Table 1. Microgrid Constant Parameters.

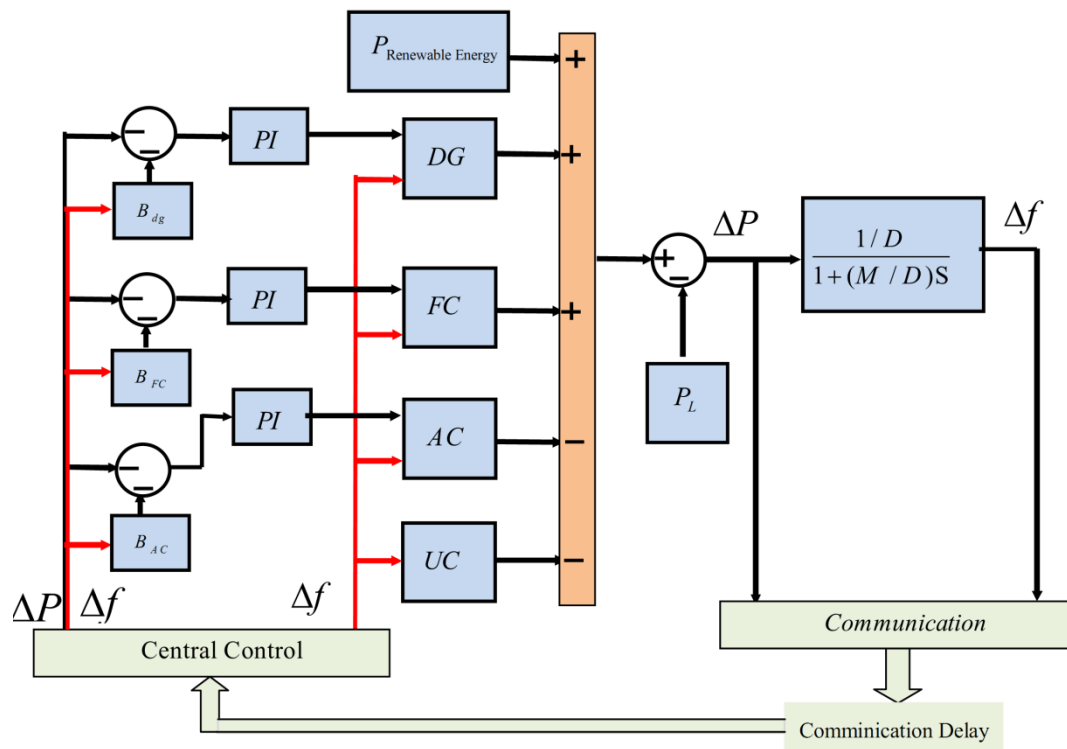| Parameter	Value	Parameter	Value
T_{uc}	0.2 (s)	T_{FC}	4 (s)
H	5 (s)	T_{AC}	0.2 (s)
D	0.012 (pu/Hz)	T_{dt}	20 (s)
T_{dg}	2 (s)	f_{base}	50 Hz

Figure 1. Illustration of the Control Units of the Studied Microgrid.

2.1. Modeling the Power Source of Diesel Generator

The diesel generators are used to compensate the power required by the microgrid by using a governor and a speed drop system. The governor controls the fuel input of the fuel engine by adjusting the fuel throttle mechanism. The gasoline or gas engine acts as a turbine and moves a synchronous generator. The diesel generator governor can be modeled by a first-order conversion function that is described in Equation (1).

$$G_{dgs}(s) = \frac{1}{1 + sT_{dgs}} \qquad (1)$$

Similarly, the turbine of this generator is also modeled by the first order conversion function.

$$G_{dt}(s) = \frac{1}{1 + sT_{dt}} \qquad (2)$$

Due to the series performance of the mechanical and electrical unit of the diesel generator, the general conversion function is as follows.

$$G_{dgt}(s) = \frac{1}{1 + sT_{dgs}} \times \frac{1}{1 + sT_{dt}} \qquad (3)$$

The control commend to the diesel generator cannot be transferred to its output immediately because of the inherent delay of mechanical systems and generation rate constraint (GRCs). Therefore, these limitations are also applied to the Diesel Dynamic Model. The complete dynamic model of the diesel generator is shown in Figure 2.
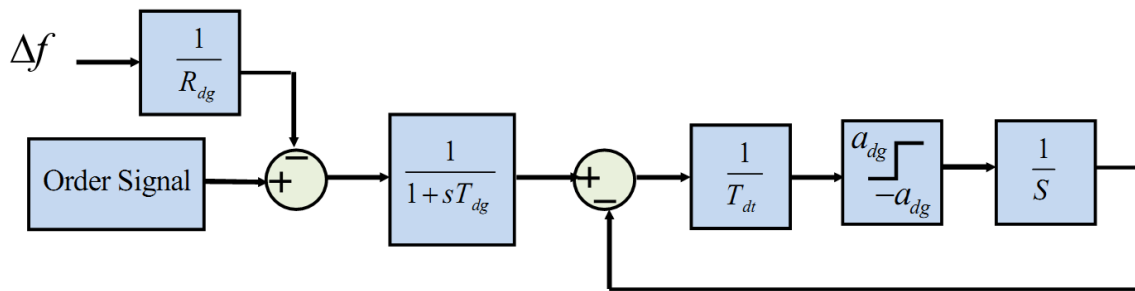
Figure 2. Dynamic Model of the Diesel Generator [33].

2.2. Fuel Cell

The fuel cell is one of the static power generation equipment that converts the chemical energy stored in hydrogen into DC electrical energy. When the generated power of the renewable energy source is less than the power required for electric loads or the consumption of loads at their peak, the fuel cell begins to generate power by injecting hydrogen stored in its hydrogen tank. Since the ultimate performance of this system is similar to the voltage source inverter, the transfer function of this power source will be in the form of the first-order model as follows:

$$G_{fc}(s) = \frac{1}{1 + sT_{fc}} \tag{4}$$

The generated power and its increase rate limit are also applied for the fuel cell. The dynamic model of a fuel cell is illustrated in Figure 3.
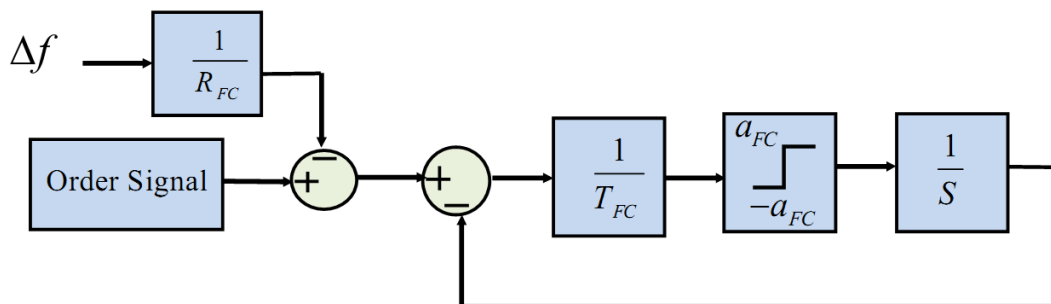

Figure 3. Dynamic Model of the Fuel Cell [33].

2.3. Electrolyze Unit

An electrolyze unit is a form of equipment that stores the extra energy of renewable energy sources. Water is decomposed into hydrogen and oxygen by passing the current between two separated electrodes. The hydrogen produced in the chemical reaction is stored in a tank and used as fuel for a fuel cell to meet load demand.

The water electrolyzes unit acts as a DC voltage source and requires a VSC inverter to be connected to a microgrid. Consequently, the transfer function will be as follows:

$$G_{AE}(s) = \frac{K_{AE}}{1 + sT_{AE}} \tag{5}$$

The power generation rate limits are also considered in the water electrolyze model. Figure 4 shows the dynamic model of the electrolyze unit.
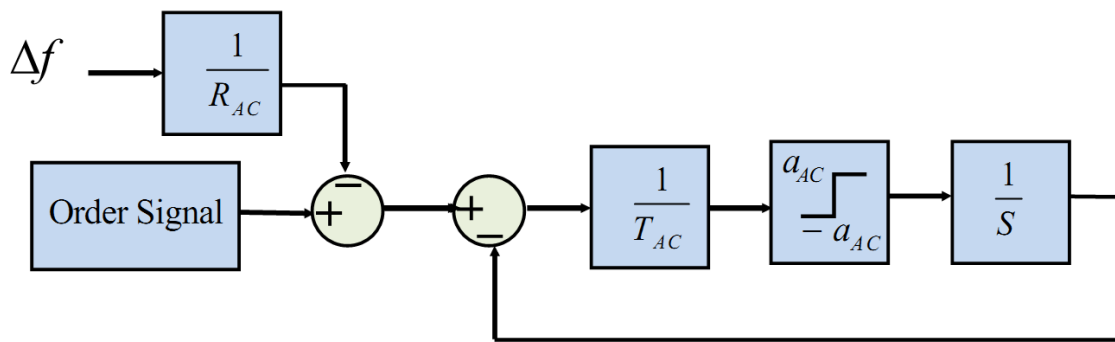
Figure 4. Dynamic Model of the Electrolyzer [33].

2.4. Model of Renewable Energy Sources

In case of renewable energies, the MPPT strategy is implemented, so controllability will not be possible for wind/PV power generation [6,7]. These systems are not participating in frequency control.

2.5. Ultra-Capacitor

The Ultra-capacitors plays an important role in increasing the virtual inertia of the network, either by power injection or by absorption. The network exchange power of the Ultra-capacitor is directly related to the derivation of frequency fluctuations. These units have very little delay in response to frequency oscillations. Thus, the dynamic model of ultra-capacitors can be illustrated in Figure 5 [27].
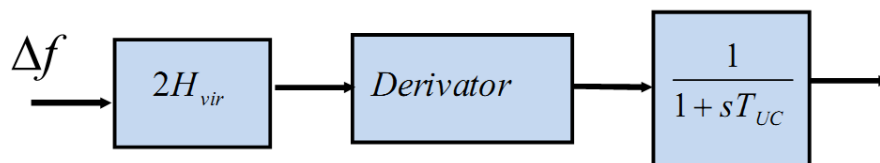

Figure 5. Dynamic Model of Ultra-capacitor.

2.6. Telecommunication System Delay

The telecommunication system is used to transfer microgrid information to the central controller. In reference [34], a first order transfer function is considered for measurement of a delay that covers the communication delay. Therefore, for the simplification of analyses, all delays in communication units modeled as the first-order function in this paper, which is expressed in Equation (6). It should be noted that any other time delay model can be used and the optimizing algorithm can determine the optimum parameters of the selected model.

$$G_{Commu}(s) = \frac{1}{1 + sT_{commu}} \tag{6}$$

2.7. Optimization Algorithm

The NSGA-II algorithm is used in this paper. The first goal is reducing the frequency fluctuations of the microgrid. Equation (7) is considered for this aim. The algorithm attempts to minimize (7) so the frequency oscillation will be in a minimum state. In addition, the second goal is determining the minimum ultra-capacitor size and the delay value of telecommunication systems to reduce the microgrid infrastructure cost. For a low ultra-capacitor size and the high delay value of telecommunication systems, the operation cost will be low. These two goals are expressed in two separate objective functions as below:

$$IAE = \sum_{i=1}^{N} |\Delta f|_i + |f|_i. \tag{7}$$

$$CostF = \left(H_{Vir\_average} - H\right) + \frac{T_{d\_avarge}}{T_d} = H_{Vir} + \frac{T_{d\_avarge}}{T_d} \tag{8}$$

In the above Equations, i.e., (7) and (8), Δf stands for frequency fluctuations, H_{Vir} is the virtual inertia, T_d is the delay of telecommunication systems, T_{d_avarge} is an average delay of telecommunication systems, and N is the number of samples in the simulation process.

The accuracy of resources and microgrid frequency response models has been investigated in the previous literature. These models have been used for the optimization process. The upper and lower limits of the decision variables of the optimization problem are listed in Table 2.

Table 2. The parameters limitation ranges.

Parameter	Limitation	Parameter	Limitation
$H_{Vir\_average}$	5–8	B_{fc}	0.05–0.3
kp_{dg}	0.1–1	R_{fc}	10–20
ki_{dg}	0.001–0.005	kp_{ac}	60–80
B_{dg}	0.07–0.2	ki_{ac}	0.01–0.5
R_{dg}	10–20	B_{ac}	0.1–3
k_{pfc}	0.01–0.3	T_{ac}	10–20
ki_{fc}	0.001–0.005	T_d	1–10

The NSGA-II algorithm, like the conventional genetic algorithm, uses mutation and crossover operators at each stage. The algorithm uses repetitive loops to obtain the optimum population. The set of solutions for the right choice must first be ranked and each solution with fewer ratings is a better solution. This algorithm also begins its operation with the initial population, based on the values of the fitness functions. The solutions are ranked with the use of the mechanism of crowding distance and dominance, and based on this, a new population is generated with crossover and mutation functions [35]. As long as the two objective functions reach convergence, the algorithm should be continued. Figure 6 shows the convergence of these two conflicting functions in the the optimization algorithm steps.The multi-objective optimization is implemented in MATLAB/SIMULINK software
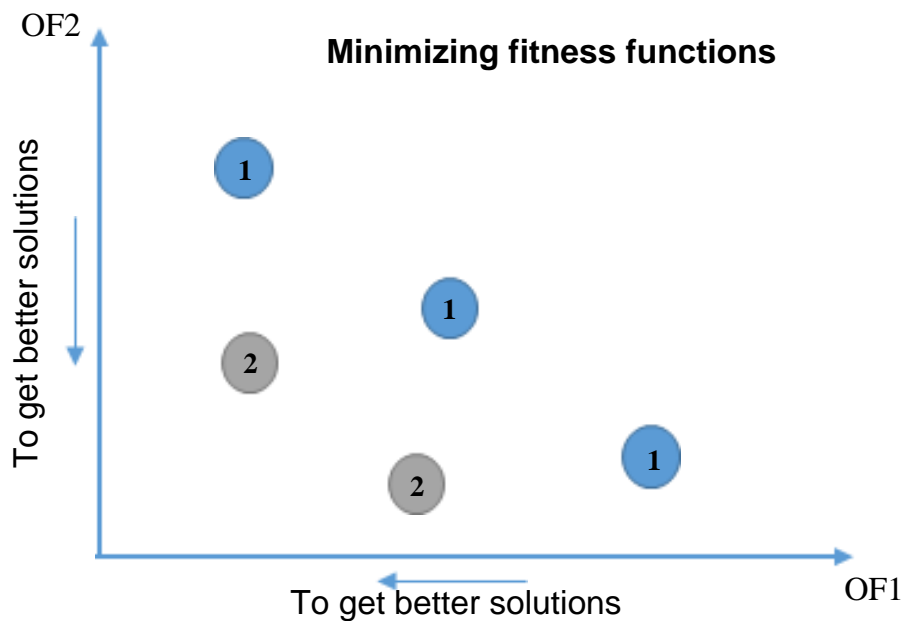

Figure 6. Pareto-based optimum solutions selection in the multi-objective optimization process.

3. Simulation Results

The frequency control system implemented in the MATLAB / SIMULINK software. The system parameters are obtained using the NSGA-II algorithm. The NSGA-II algorithm is used to optimize two conflict objectives, i.e. operation cost reduction and frequency oscillation reduction. The optimizing processes are showed as Pareto curves. The final Pareto curve is shown in Figure 7. The selected solution presented in the Pareto curve is considered an equally good solution. Low frequency oscillation with low operation costs can be derived in the selected point. The parameters values for the selected solution listed in Table 3. The optimum and non-optimum values are listed in Table 3. The non-optimum parameters were obtained by the trial and error method, reducing the infrastructure costs. The system was simulated in three scenarios:

✓ Scenario I: In the first scenario, the performance of the microgrid was simulated through the application of a telecommunication networks delay with non-optimum parameter values.
✓ Scenario II: In the second scenario, the performance of the microgrid with the optimum control parameters, virtual inertia and telecommunication systems delay values is verified through simulation setups.
✓ Scenario III: In the third scenario, the delay of the telecommunication system is not considered while the optimum parameters are applied in the simulated system.
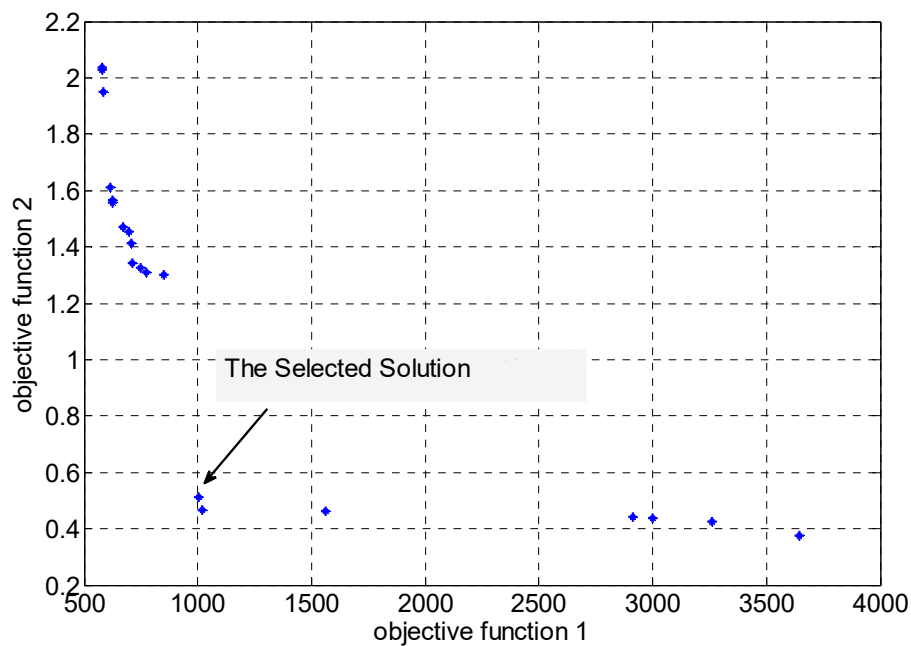

Figure 7. Frontiers of Pareto of the two objective functions drawn from NSGA-II optimization.

Table 3. Optimum and non-optimum parameters of the control system, ultra-capacitor size, and telecommunications system delay values.

Non-Optimum Parameters		Optimum Parameters	
Parameter	Value	Parameter	Value
$Hvir$	1	$Hvir$	0.2005
kp_{dg}	0.244	kp_{dg}	0.7167
ki_{dg}	0.0032	ki_{dg}	0.0024
B_{dg}	0.1386	B_{dg}	0.1687
R_{dg}	19.93	R_{dg}	17.084
kp_{fc}	0.0298	kp_{fc}	0.0764
ki_{fc}	0.0043	ki_{fc}	0.0025
B_{fc}	0.1878	B_{fc}	0.2338
R_{fc}	17.09	R_{fc}	12.7212
kp_{ac}	57.7635	kp_{ac}	75.3
ki_{ac}	7.08	ki_{ac}	0.4
B_{ac}	0.5923	B_{ac}	0.1
R_{ac}	28.1	R_{ac}	16.1
T_d	3	T_d	4.8
$CostF$	1.2	$CostF$	0.513

These scenarios show the effectiveness of the selected solution in overcoming frequency oscillation. In all the scenarios, the load and renewable energy source step changes are considered in the same profile. The magnitude of the load demand is equal to 1/1 per unit. When the simulation time reaches 1500 (s), it will reach 0.9 per unit. In contrast, the generation of renewable energy units is equal to one per unit. The frequency behavior of the microgrid in this section is shown in Figure 8. The microgrid frequency fluctuation has decreased with the application of optimum parameters and can be clearly seen in Figure 8. Meanwhile, the telecommunication system delay increases the undershoot and settling time of the frequency fluctuation. Up to t = 1500 s, diesel generator and fuel cell are expected to generate power, and after this instance the electrolysis unit is expected to absorb unbalanced power. The dynamic responses of the power sources and the electrolyze unit, while applying the optimum parameters, can be investigated using simulation results. Output powers of the source for the diesel generator, the fuel cell, and the electrolyze unit are shown in Figures 9–11, respectively. As can be seen from these figures, the electrolysis unit and diesel generator have the fastest and the slowest dynamic behavior responses, respectively. In the initial simulation time, the fuel cell injects power to grid with a high rate to compensate frequency drooping. Up to t = 1500 s, in steady state condition, the diesel generator and fuel cell contribute in power balancing and frequency stability.

Due to the high penetration of renewable energy sources, the actual inertia of the microgrid systems is small. This phenomenon shows its effect on steady frequency oscillation and high overshoot and undershoots in microgrid frequency responses. By increasing the communication delay, the stability margin of the microgrid can be improved. By increasing the microgrid inertia by increasing the virtual inertia value, the microgrid frequency is made less sensitive to the increasing commendation time delay. The studied microgrid behavior, for a different time delay value, is stable under the special condition that is shown in Figure 12. Two areas are distinguished in this figure. For a given H_{vir} value, if the time delay value is in the blue area, the system will be stable. The maximum virtual inertia margin that guarantees the stability is shown in Figure 13. To derive Figures 10 and 11, the conventional repetition process is used. The virtual inertia and time delay step changes are considered as being 0.5 Hz and 0.025 s, respectively.

With respect to general load and power generation profile, shown in Figure 14, the frequency behaviour of the grid while applying the variable profiles of the load power and power generated by renewable energy sources is shown in Figure 14. The frequency behavior of the grid with optimum

parameters (Figure 15) shows that the proposed strategy is more effective than the non-optimum based controller in damping frequency oscillation.
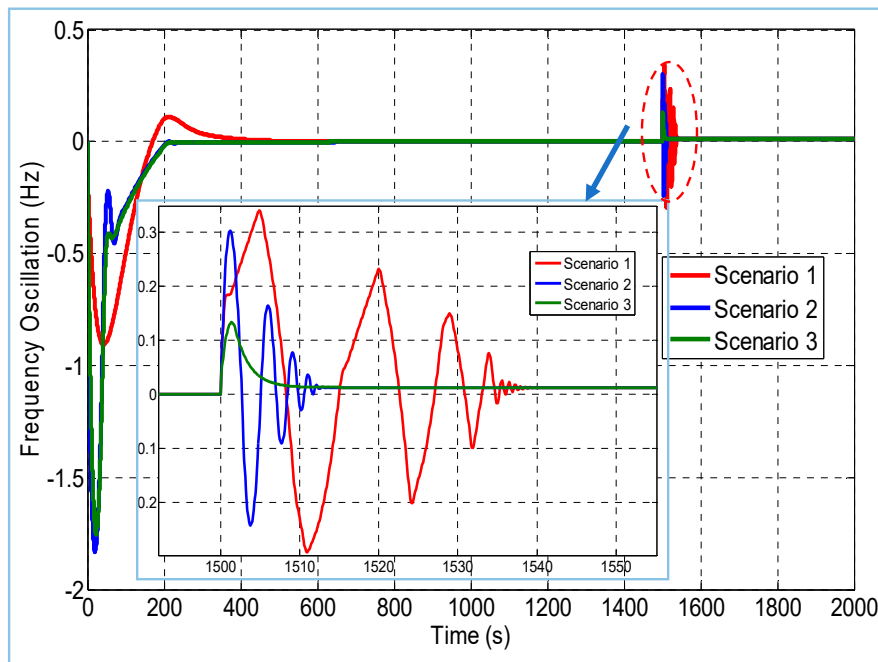

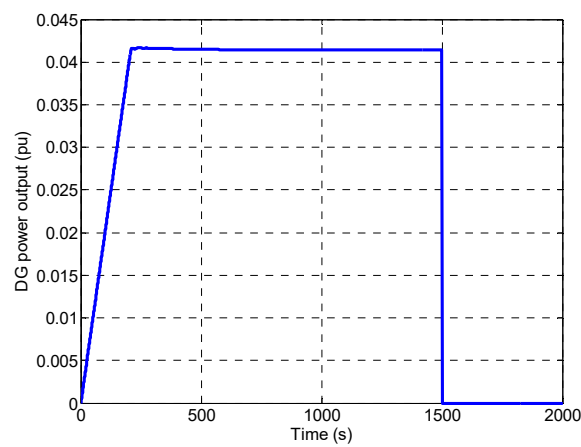**Figure 8.** Comparison of the microgrid responses in terms of frequency in three scenarios.
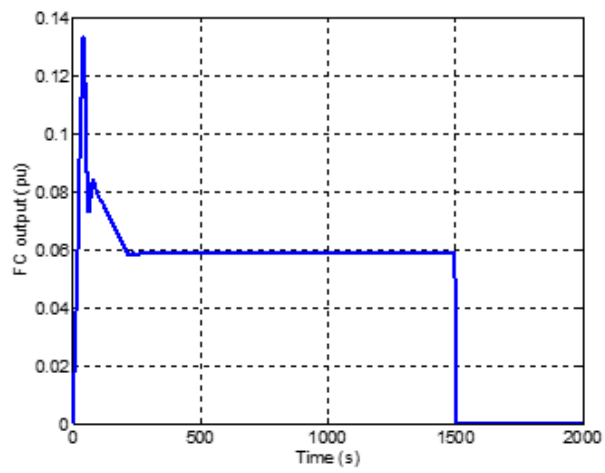

Figure 9. The diesel Generator output power.
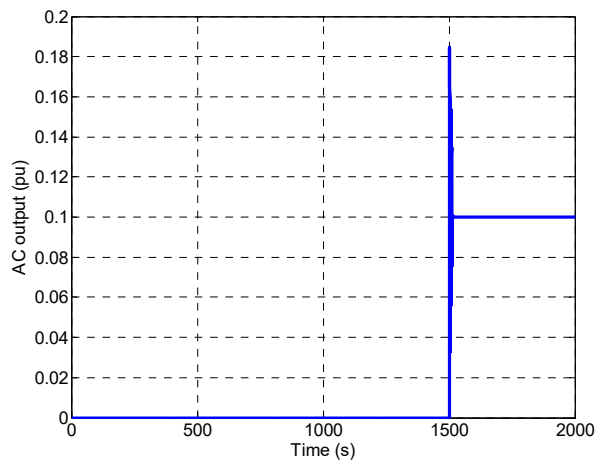
Figure 10. The fuel cell output power.
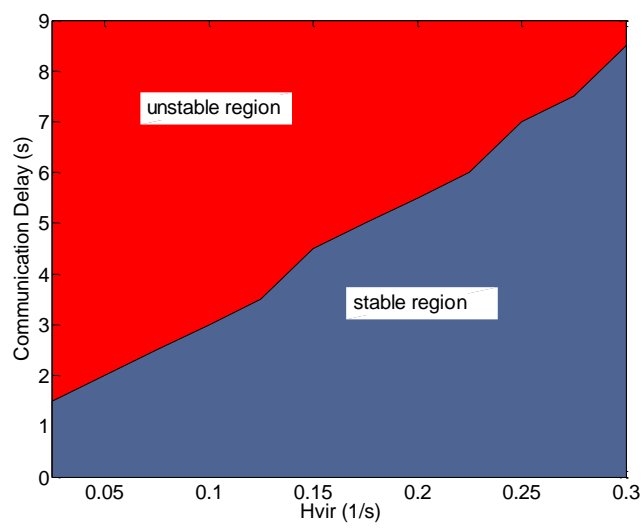

Figure 11. The electrolyzer output power.

Figure 12. The stable and unstable regains for the studied microgrid.
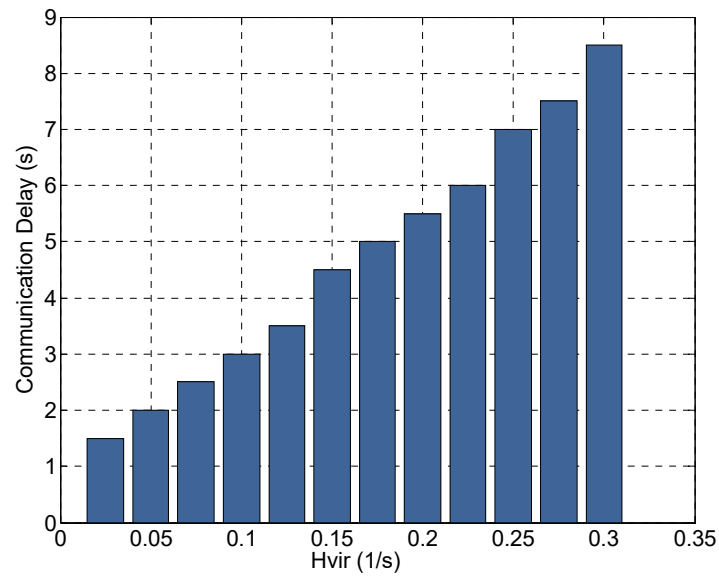
Figure 13. The maximum acceptable communication delay for given virtual values.
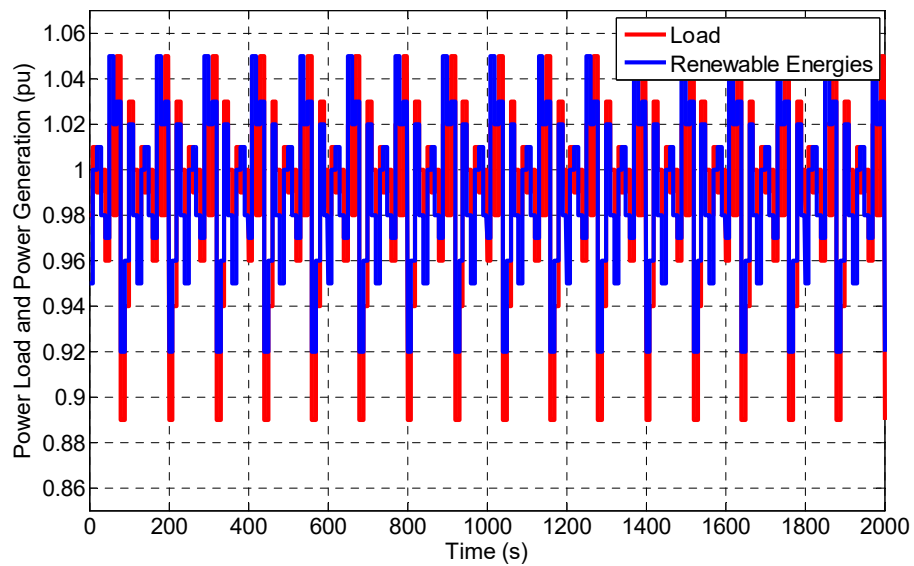

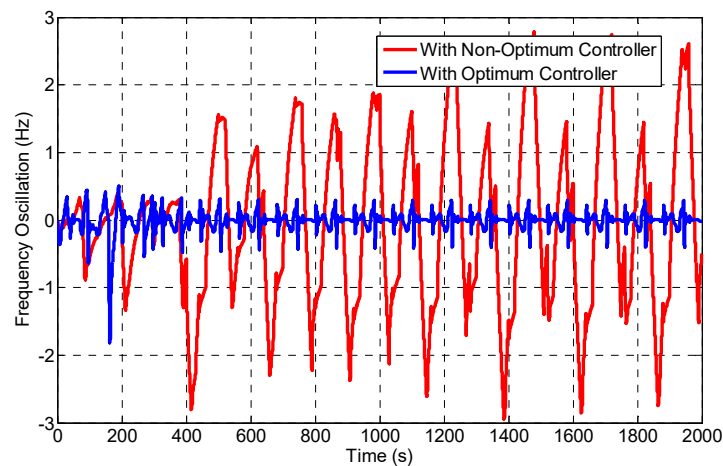**Figure 14.** The renewable energy output and load demand powers.

Figure 15. Frequency deviation with optimum and non-optimum controllers.

In real grids, the output power of the renewable energy sources and load power consumption are stochastic. In this paper, the Gaussian distributions are assumed for the random output of the renewable energy sources and load profile, which expressed mathematically in Equations (9) and (10), respectively.

$$g_1(x) = \frac{1}{\sqrt{0.0005}} \exp\left(\frac{-1}{2}\left(\frac{x-1}{\sqrt{0.0005}}\right)^2\right) \tag{9}$$

$$g_2(x) = \frac{1}{\sqrt{0.001}} \exp\left(\frac{-1}{2}\left(\frac{x-1}{\sqrt{0.001}}\right)^2\right) \tag{10}$$

The frequency behavior of a microgrid while applying the specific uncertainties, optimum and non-optimum parameters is simulated and the results of these simulations are shown in Figure 16. The optimum-based controller can overcome power-unbalancing events and stabilize the frequency.
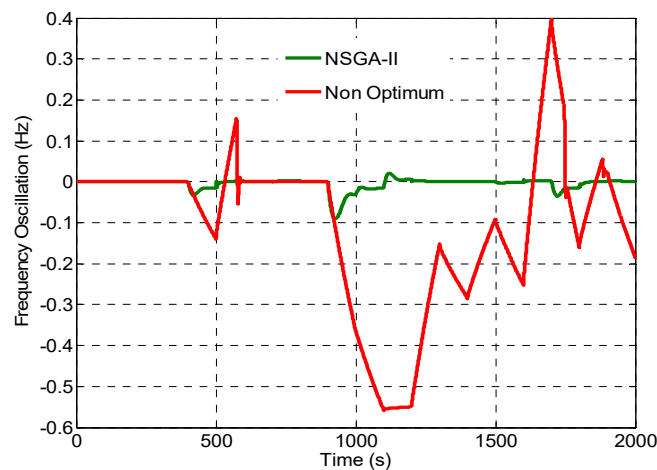
Figure 16. Frequency deviation under uncertainties.

4. Conclusions

A microgrid with controllable and uncontrollable sources, including solar, wind, a diesel generator, fuel cell, and an electrolyze unit, was investigated in this paper. The frequency stability of the grid was investigated while considering the ultra-capacitor unit and time delay of communication systems. The communication delay decreases the system function's ability to control the frequency. In this paper, tuning the virtual inertia constant and the time delay value in the communication

together with the parameters of the load-frequency controllers of the power sources was considered to improve the frequency stability of low inertia microgrids with the presence of the time delay in the communication network. In fact, the best way to tune these unknown parameters has been determined as a multi-objective optimization problem (NSGA-II algorithm), which considers both frequency stability and economic concerns. Reducing delay in telecommunication systems and increasing virtual inertia values, while applying the ultra-capacitor, can improve the damping of frequency fluctuations; however, it also increases the cost of grid operation. With the tuning of the control system parameters, time delay value and the virtual inertia value, the aforementioned challenges are solved. In the studied microgrid, the simulation was performed in MATLAB/Simulink numerical software. Investigation results prove the effectiveness of this network strategy to overcome frequency fluctuations.

References

1. Hatziargyriou, N. (Ed.) *Microgrids: Architectures and Control*; John Wiley & Sons: Hoboken, NJ, USA, 2014.
2. Liu, W.; Gu, W.; Sheng, W.; Meng, X.; Wu, Z.; Chen, W. Decentralized multi-agent system-based cooperative frequency control for autonomous microgrids with communication constraints. *IEEE Trans. Sustain. Energy* **2014**, *5*, 446–456. [CrossRef]
3. Abdel-Hamed, A.M.; Ellissy, A.E.E.K.; El-Wakeel, A.S.; Abdelaziz, A.Y. Optimized control scheme for frequency/power regulation of microgrid for fault tolerant operation. *Electr. Power Compon. Syst.* **2016**, *44*, 1429–1440. [CrossRef]
4. Venkataramanan, G.; Marnay, C. A larger role for microgrids. *IEEE Power Energy Mag.* **2008**, *6*, 78–82. [CrossRef]
5. Chen, C.; Wang, J.; Qiu, F.; Zhao, D. Resilient distribution system by microgrids formation after natural disasters. *IEEE Trans. Smart Grid* **2016**, *7*, 958–966. [CrossRef]
6. Tani, A.; Camara, M.B.; Dakyo, B. Energy management in the decentralized generation systems based on renewable energy—Ultracapacitors and battery to compensate the wind/load power fluctuations. *IEEE Trans. Ind. Appl.* **2015**, *51*, 1817–1827. [CrossRef]
7. Ahmed, N.A.; Miyatake, M.; Al-Othman, A.K. Power fluctuations suppression of stand-alone hybrid generation combining solar photovoltaic/wind turbine and fuel cell systems. *Energy Convers. Manag.* **2008**, *49*, 2711–2719. [CrossRef]
8. Chen, Z.; Spooner, E. Grid power quality with variable speed wind turbines. *IEEE Trans. Energy Convers.* **2001**, *16*, 148–154. [CrossRef]
9. Liang, X. Emerging power quality challenges due to integration of renewable energy sources. *IEEE Trans. Ind. Appl.* **2017**, *53*, 855–866. [CrossRef]
10. Díaz-González, F.; Sumper, A.; Gomis-Bellmunt, O.; Villafáfila-Robles, R. A review of energy storage technologies for wind power applications. *Renew. Sustain. Energy Rev.* **2012**, *16*, 2154–2171. [CrossRef]
11. Shim, J.W.; Cho, Y.; Kim, S.J.; Min, S.W.; Hur, K. Synergistic control of SMES and battery energy storage for enabling dispatchability of renewable energy sources. *IEEE Trans. Appl. Supercond.* **2013**, *23*, 5701205. [CrossRef]
12. Onar, O.C.; Uzunoglu, M.; Alam, M.S. Dynamic modeling, design and simulation of a wind/fuel cell/ultra-capacitor-based hybrid power generation system. *J. Power Sources* **2006**, *161*, 707–722. [CrossRef]
13. Jing, W.; Lai, C.H.; Wong, W.S.; Wong, M.D. Dynamic power allocation of battery-supercapacitor hybrid energy storage for standalone PV microgrid applications. *Sustain. Energy Technol. Assess.* **2017**, *22*, 55–64. [CrossRef]
14. Chandrakala, V.; Sukumar, B.; Sankaranarayanan, K. Load frequency control of multi-source multi-area hydro thermal system using flexible alternating current transmission system devices. *Electr. Power Compon. Syst.* **2014**, *42*, 927–934. [CrossRef]

15. Arani, M.F.M.; Mohamed, Y.A.R.I. Cooperative control of wind power generator and electric vehicles for microgrid primary frequency regulation. *IEEE Trans. Smart Grid* **2018**, *9*, 5677–5686. [CrossRef]

16. Liu, Y.; You, S.; Tan, J.; Zhang, Y.; Liu, Y. Frequency Response Assessment and Enhancement of the US Power Grids toward Extra-High Photovoltaic Generation Penetrations—An Industry Perspective. *IEEE Trans. Power Syst.* **2018**, *33*, 3438–3449. [CrossRef]

17. Kalantar, M. Dynamic behavior of a stand-alone hybrid power generation system of wind turbine, microturbine, solar array and battery storage. *Appl. Energy* **2010**, *87*, 3051–3064. [CrossRef]

18. Gao, L.; Jiang, Z.; Dougal, R.A. An actively controlled fuel cell/battery hybrid to meet pulsed power demands. *J. Power Sources* **2004**, *130*, 202–207. [CrossRef]

19. Nayeripour, M.; Hoseintabar, M.; Niknam, T. Frequency deviation control by coordination control of FC and double-layer capacitor in an autonomous hybrid renewable energy power generation system. *Renew. Energy* **2011**, *36*, 1741–1746. [CrossRef]

20. Khooban, M.H.; Niknam, T.; Blaabjerg, F.; Dragičević, T. A new load frequency control strategy for micro-grids with considering electrical vehicles. *Electr. Power Syst. Res.* **2017**, *143*, 585–598. [CrossRef]

21. Sigrist, L.; Egido, I.; Miguélez, E.L.; Rouco, L. Sizing and controller setting of ultracapacitors for frequency stability enhancement of small isolated power systems. *IEEE Trans. Power Syst.* **2015**, *30*, 2130–2138. [CrossRef]

22. Yang, T.; Zhang, Y.; Wang, Z.; Pen, H. Secondary frequency stochastic optimal control in independent microgrids with virtual synchronous generator-controlled energy storage systems. *Energies* **2018**, *11*, 2388. [CrossRef]

23. Hammad, E.; Farraj, A.; Kundur, D. On Effective Virtual Inertia of Storage-Based Distributed Control for Transient Stability. *IEEE Trans. Smart Grid* **2019**. Accepted for publications. [CrossRef]

24. Alipoor, J.; Miura, Y.; Ise, T. Power system stabilization using virtual synchronous generator with alternating moment of inertia. *IEEE J. Emerg. Sel. Top. Power Electron.* **2015**, *3*, 451–458. [CrossRef]

25. Kerdphol, T.; Rahman, F.; Mitani, Y.; Hongesombut, K.; Küfeoğlu, S. Virtual inertia control-based model predictive control for microgrid frequency stabilization considering high renewable energy integration. *Sustainability* **2017**, *9*, 773. [CrossRef]

26. Fang, J.; Li, H.; Tang, Y.; Blaabjerg, F. Distributed power system virtual inertia implemented by grid-connected power converters. *IEEE Trans. Power Electron.* **2018**, *33*, 8488–8499. [CrossRef]

27. Jiang, L.; Yao, W.; Wu, Q.H.; Wen, J.Y.; Cheng, S.J. Delay-dependent stability for load frequency control with constant and time-varying delays. *IEEE Trans. Power Syst.* **2012**, *27*, 932–941. [CrossRef]

28. Liu, S.; Wang, X.; Liu, P.X. Impact of Communication Delays on Secondary Frequency Control in an Islanded Microgrid. *IEEE Trans. Ind. Electron.* **2015**, *62*, 2021–2031. [CrossRef]

29. Singh, V.P.; Kishor, N.; Samuel, P. Load frequency control with communication topology changes in smart grid. *IEEE Trans. Ind. Inform.* **2016**, *12*, 1943–1952. [CrossRef]

30. Wang, H.; Zeng, G.; Dai, Y.; Bi, D.; Sun, J.; Xie, X. Design of a Fractional Order Frequency PID Controller for an Islanded Microgrid: A Multi-Objective Extremal Optimization Method. *Energies* **2017**, *10*, 1502. [CrossRef]

31. Chaine, S.; Tripathy, M.; Satpathy, S. NSGA-II based optimal control scheme of wind thermal power system for improvement of frequency regulation characteristics. *Ain Shams Eng. J.* **2015**, *6*, 851–863. [CrossRef]

32. Kamjoo, A.; Maheri, A.; Dizqah, A.M.; Putrus, G.A. Multi-objective design under uncertainties of hybrid renewable energy system using NSGA-II and chance constrained programming. *Int. J. Electr. Power Energy Syst.* **2016**, *74*, 187–194. [CrossRef]

33. Mishra, S.; Mallesham, G.; Jha, A.N. Design of controller and communication for frequency regulation of a smart microgrid. *IET Renew. Power Gener.* **2012**, *6*, 248–258. [CrossRef]

34. Abazari, A.; Monsef, H.; Wu, B. Coordination strategies of distributed energy resources including FESS, DEG, FC and WTG in load frequency control (LFC) scheme of hybrid isolated micro-grid. *Int. J. Electr. Power Energy Syst.* **2019**, *1*, 535–547. [CrossRef]

35. Deb, K.; Pratap, A.; Agarwal, S.; Meyarivan, T.A.M.T. A fast and elitist multiobjective genetic algorithm: NSGA-II. *IEEE Trans. Evol. Comput.* **2002**, *6*, 182–197. [CrossRef]